Progress in Biophysics and Molecular Biology 130 (2017) 333–343

Contents lists available at ScienceDirect

Progress in Biophysics and Molecular Biology

journal homepage: www.elsevier.com/locate/pbiomolbio

Original Research

Load-dependent effects of apelin on murine cardiomyocytes

Rémi Peyronnet [a, b, *, 1], Christian Bollensdorff [b, c, 1], Rebecca A. Capel [d, 1], Eva A. Rog-Zielinska [a, b], Christopher E. Woods [e, f], David N. Charo [e], Oleg Lookin [g], Giovanni Fajardo [e], Michael Ho [e], Thomas Quertermous [e], Euan A. Ashley [e], Peter Kohl [a, b]

[a] Institute for Experimental Cardiovascular Medicine, University Heart Centre Freiburg · Bad Krozingen, Medical School of the University of Freiburg, Germany
[b] Imperial College London, NHLI, Heart Science Centre, UK
[c] Sidra Medical and Research Center, Qatar Foundation, Qatar
[d] Department of Pharmacology, University of Oxford, UK
[e] Stanford University Division of Cardiovascular Medicine, Stanford, USA
[f] Palo Alto Medical Foundation, Burlingame, CA, USA
[g] Ural Branch of the Russian Academy of Sciences, Ekaterinburg, Russian Federation

ARTICLE INFO

Article history:
Received 13 August 2017
Received in revised form
7 September 2017
Accepted 8 September 2017
Available online 18 September 2017

Keywords:
Carbon fibres
Stretch
Frank-Starling Gain
Contractility
Lusitropy

ABSTRACT

The apelin peptide is described as one of the most potent inotropic agents, produced endogenously in a wide range of cells, including cardiomyocytes. Despite positive effects on cardiac contractility in multicellular preparations, as well as indications of cardio-protective actions in several diseases, its effects and mechanisms of action at the cellular level are incompletely understood.

Here, we report apelin effects on dynamic mechanical characteristics of single ventricular cardiomyocytes, isolated from mouse models (control, apelin-deficient [Apelin-KO], apelin-receptor KO mouse [APJ-KO]), and rat. Dynamic changes in maximal velocity of cell shortening and relaxation were monitored. In addition, more traditional indicators of inotropic effects, such as maximum shortening (in mechanically unloaded cells) or peak force development (in auxotonic contracting cells, preloaded using the carbon fibre technique) were studied.

The key finding is that, using Apelin-KO cardiomyocytes exposed to different preloads with the 2-carbon fibre technique, we observe a lowering of the slope of the end-diastolic stress-length relation in response to 10 nM apelin, an effect that is preload-dependent. This suggests a positive lusitropic effect of apelin, which could explain earlier counter-intuitive findings on an apelin-induced increase in contractility occurring without matching rise in oxygen consumption.

1. Introduction

Cardiac muscle possesses a highly-developed intrinsic ability to auto-regulate its function, thereby matching performance of the heart to systemic circulatory demand. In cardiac disease, this self-regulatory ability of the heart is blunted. Correcting auto-regulation and steadying cardiac output are major goals of pharmacological interventions.

The vast majority of drug studies *in vitro*, especially those using single cardiomyocytes, do not account for the mechanical environment, which *in situ* not only imposes a constantly changing external demand, but is associated with cell strain even in the diastolic (resting) state of myocardium (Bub et al., 2010). Due to this, drug effects that depend on, or are modulated by, the mechanical environment may be missed in standard *in vitro* studies. The 2-carbon fibre (CF) technique (Le Guennec et al., 1990) offers an experimental approach to controlling the mechanical environment of isolated cells. It can be used therefore to explore drug effects under different mechanical loads.

Apelin was identified in 1998 as a specific ligand for the apelin receptor (APJ), until then classed as an 'orphaned' G-protein coupled receptor (Tatemoto et al., 1998a). In human, mouse and rat the gene encoding apelin incorporates 3 exons and is located on chromosome X. Human apelin shares over 80% amino acid

* Corresponding author. Institute for Experimental Cardiovascular Medicine, University Heart Centre Freiburg · Bad Krozingen, Medical School of the University of Freiburg, Germany.
E-mail address: remi.peyronnet@universitaets-herzzentrum.de (R. Peyronnet).
[1] These authors contributed equally to the work.

https://doi.org/10.1016/j.pbiomolbio.2017.09.013

Abbreviations

APJ	apelin receptor
APJ-KO	apelin receptor knock out
CF	carbon fibre
EDSLR	end diastolic stress length relation
ESSLR	end systolic stress length relation
KO	knock out
FFT	Fast Fourier Transform
FSG	Frank-Starling Gain
FSS	fractional sarcomere shortening
MABP	mean arterial blood pressure
NT	normal Tyrode solution
PK	protein kinase
RSL	resting sarcomere length
SL	sarcomere length
TAC	trans-aortic constriction
TTP	time to peak contraction
TTRel	time to 90% relaxation
VmaxCon	maximum velocity of contraction
VmaxRel	maximum velocity of relaxation
WT	wild type

sequence homology with mouse and rat, indicating a strong evolutionary conservation of the gene. Apelin orthologues are present in many species including pig, rhesus macaque, cow and zebrafish. Apelin and apelin receptor have been shown previously to be expressed in cardiomyocytes of human (Kleinz et al., 2005; Walker et al., 2014) and rodents (Ronkainen et al., 2007; Kawamata et al., 2001). Apelin is synthesised as pre-proapelin, a 77 amino acid pre-proprotein (Tatemoto et al., 2001). It is then cleaved to its active forms, of which 46 have been identified in bovine colostrum (Mesmin et al., 2011). At least four fragments are biologically important, the −12, −13, −17 and −36 amino acid proteins (O'Carroll et al., 2013). These all represent fragments of the N-terminal region of the pre-proprotein and increase in potency but decrease in receptor binding affinity as the size of fragment is reduced (Hosoya et al., 2000). Interest in the peptide, which can act as neuromediator, circulating hormone, and auto-/paracrine agent, has grown rapidly (for reviews see (Beltowski, 2006; Higuchi et al., 2007; Lee et al., 2006; Chen et al., 2016; Folino et al., 2015)). In the context of cardiovascular function, apelin demonstrates fascinating properties. It increases myocardial contractility (Berry et al., 2004) in a load-dependent manner (Szokodi et al., 2002a) apparently without triggering cardiac hypertrophy and at low metabolic cost (Ashley et al., 2005). In addition, circulating apelin lowers mean arterial blood pressure (MABP) (Lee et al., 2000). Furthermore, apelin has been shown to have cardioprotective properties, counter-balancing Angiotensin-II mediated pressor effects (Buettner et al., 2007; Ishida et al., 2004) and reducing myocardial infarct size (Simpkin et al., 2007). Apelin concentration is increased in obese patients (Buettner et al., 2007) (which may help to explain why obesity is a positive predictor of survival after revascularisation) and during early stages of heart failure (Chen et al., 2003). In addition, its synthesis is activated in patho-physiological hotspots by hypoxia inducible factors (which may add to the complexity of interpretation of single cell data, whose isolation may involve hypoxic periods) (Ronkainen et al., 2007).

There is no shortage of at least partially contradictory results. These include transient (Farkasfalvi et al., 2007) *vs.* bi-phasic (Charles et al., 2006) responses to apelin application; 10^2–10^3 fold differences in apelin concentrations required to achieve sub-maximal effects in patho-physiologically remodelled individuals of the same species (Lee et al., 2005), pronounced circadian discrepancies in physiological responses to apelin (O'Shea et al., 2003), and route-of-application dependencies (such as MABP reduction when apelin is applied peripherally (Tatemoto et al., 2001; Cheng et al., 2003) *vs.* MABP increase upon intra-cerebroventricular application (Kagiyama et al., 2005; Seyedabadi et al., 2002).

Nonetheless, even based on the most cautious assessment of available information, it remains that apelin is the most potent endogenous inotrope: the half maximal effective concentration (EC_{50}) is 33 pmol·L^{-1} in isolated heart (Szokodi et al., 2002a). Its ability to lower MABP, increase ejection fraction, and reduce end-diastolic cardiac dimensions significantly improves cardiac efficiency (Ashley et al., 2005). In addition, by increasing active force production in a preload dependent manner (Szokodi et al., 2002a; Ashley et al., 2005), it may hold an exciting key to pharmacological targeting of diseased tissue (which is often less contractile, and thus exposed to more pronounced preload-related strain), without a need for local drug delivery or other targeting measures.

Investigation of direct apelin effects on cardiac muscle is difficult *in situ*, not only because of the presence of multiple interacting regulatory pathways (including effects on circulating messengers and nervous system-mediated responses), but also because apelin is endogenously synthesised in many cardiac cell types, including endothelial cells, adipocytes, and coronary smooth muscle, all of whom may exert paracrine influences on cardiomyocytes. This highlights the value of performing single cardiomyocyte studies.

In this study we analyse apelin effects on cell contractile parameters in mechanically unloaded, preloaded and after-loaded cells, isolated from control, apelin deficient (Apelin-KO) and apelin receptor KO mice (APJ-KO) hearts. The non-dimensional Frank-Starling Gain (FSG) index (Bollensdorff et al., 2011), a contractility parameter that is independent of cell cross-section (which aids inter-individual comparisons), is used for evaluation.

2. Material and methods

Experiments were performed on wild type C57BL/6 mice, wild type Sprague Dawley rats, and genetically modified mice: Apelin-KO and APJ-KO (described elsewhere (Charo et al., 2009)), all at 8–12 weeks of age. The apelin gene is located on the X-chromosome, so male mice were used.

The apelin used for pharmacological interventions was a pyroglutamyl form of apelin-13 from American Peptide Company Inc., Sunnyvale, USA; (Glp1) apelin 13, Human, Bovine 12-1-16, Lot T11108A1. This isoform was chosen because it has been reported to be the most potent (Kawamata et al., 2001; Hosoya et al., 2000; Tatemoto et al., 1998b; Medhurst et al., 2003) and also because it is the predominant form found in the human heart (Maguire et al., 2009). We utilised 10 nM to match previous single cell experiments (Farkasfalvi et al., 2007). This is high enough to produce a sub-maximal response, based on previous dose-response reports in the literature (Szokodi et al., 2002a; Cheng et al., 2013).

2.1. Single cell isolation

All experiments were conducted in accordance with the guidelines of relevant institutional animal care committees and with ethics regulations, in agreement with the UK Home Office Animals (Scientific Procedures) Act of 1986. All chemicals were purchased from Sigma Aldrich, UK, unless otherwise stated.

2.1.1. Mice

Murine cardiomyocyte isolation (N = 59 hearts) has been described elsewhere (Louch et al., 2011). In brief: after Schedule 1

killing the heart was swiftly excised and mounted to a Langendorff perfusion system at 37 °C. The heart was perfused during the first 2–3 min with Normal Tyrode (NT) solution, containing (in mM): NaCl 140, KCl 6, $CaCl_2$ 1, $MgCl_2$ 1, HEPES 10, glucose 10 (pH 7.4) to help clearing the vessels and to confirm presence of regular spontaneous contractions. Then a cardioplegic low calcium (45 μM) solution was perfused for 5 min, followed by the enzyme solution using the following buffer (in mM): NaCl 120, KCl 14.7, $CaCl_2$ 0.2, $MgSO_4$ 5, sodium pyruvate 5, taurine 20, HEPES 10, glucose 5.5 (pH 7.4) and 0.6 mg/mL Collagenase II (394–405 U/mg, Worthington, Biochemical Corp., Lakewood, NJ) plus 0.4 mg/mL Hyaluronidase (digestion time 6–10 min). All solutions were maintained at 37 °C and continuously oxygenated. Digestion was stopped by adding bovine albumin serum (1 mg/mL) and remaining tissue chunks were gently dissociated mechanically using forceps for agitation (while avoiding tissue stretch) and by gently swirling the solution. Single cardiomyocytes were gradually adjusted to higher concentrations of Ca^{2+} in several steps: 100, 400, 900 μM, and 1.8 mM Ca^{2+} (in the cardioplegic solution also containing bovine albumin serum). Stock solutions were prepared in advance, glucose and calcium were added on the day of the experiment.

2.1.2. Rats

Rat ventricular myocytes were also isolated by enzymatic perfusion. Hearts from male SD rats (280–400 g, N = 5) were swiftly excised after Schedule 1 killing, cannulated *via* the aorta and Langendorff-perfused at a flow rate of 6.5 mL/min using a modified NT solution containing heparin (1 μL/mL) and (in mM) NaCl 128, KCl 2.6, $MgSO_4$ 1.18, KH_2PO_4 1.18, HEPES 10, taurine 20, glucose 11; $CaCl_2$ 1.8; pH 7.4 at room temperature to wash the coronary vasculature. The pulmonary artery was cut open to prevent pressure build-up within the heart. The heart was then perfused for 5 min with the modified NT solution containing no calcium and 0.5 mM EGTA to chelate calcium in the heart. Afterwards the modified NT solution containing 10 μM Ca^{2+} and the enzyme Liberase (Blendzyme3, Roche, Basel, Switzerland, order number 11814184001) at 10 mg in 50 mL was recirculated for 10 min through the heart. All solutions were oxygenated and heated to 37 °C. Thereafter, the ventricles were cut along the atrio-ventricular border, suspended in oxygenated modified NT solution containing 10 μM Ca^{2+}, and gently chopped into small cubes of about 2 mm^3. The solution was then filtered and the supernatant containing ventricular cells collected in 15 mL centrifugation tubes. The remaining tissue was resuspended in 10 μM Ca^{2+}-containing modified NT solution and gently agitated. The procedure was repeated up to 6 times until little or no tissue remained. The centrifuge tubes were centrifuged at 16 g (300 rpm), room temperature, for 1 min. The supernatant that contains dead cells and debris was discarded and the cells at the bottom carefully resuspended in warm solution containing (in mM) NaCl 140, KCl 5.4, $MgCl_2$ 1, HEPES 5, glucose 11, $CaCl_2$ 1.8 after gradual (100, 400, 900 μM) calcium adjustment, bovine serum albumin 1 mg/mL, and 0.83 mg trypsin inhibitor in 50 mL.

2.2. CF technique

This technique is used to apply axial stretch to cells and measure active and passive forces (Iribe et al., 2007). A pair of compliant, computer controlled and piezo positioned CF (generously supplied by Prof Jean-Yves LeGuennec; Fig. 1A–D), attached glue-free to opposite ends of the cell, are used to dynamically control the mechanical environment of isolated intact cardiomyocytes. Microstructures present at the surface of suitable CF (Fig. 1A and B) are thought to be instrumental for the attachment of the CF to the cell, whereas smooth fibres (Fig. 1C and D) do not stick to cardiomyocytes. To hold the CF, thin borosilicate capillaries were pulled from glass tubes (inner diameter: 1.16 mm; outer diameter: 2.00 mm, GC200F-10 from Harvard Apparatus Company) and a CF was mounted in the fine tip of the pulled capillary (Fig. 1E).

The narrow end of the capillary (holding a CF) was thermally bent by 45° to allow parallel alignment of fibres with the bottom of the perfusion chamber. The length of the CF protruding from the capillary was adjusted to 1.20 mm and fixed with a cyanoacrylate-adhesive.

A force transducer system (Aurora Scientific) was used to calibrate CF stiffness (range between 0.01 and 0.1 N/m). The wider end of the glass tube was mounted in the holder of a hydraulic manipulator (MW-300; Narishige, Tokyo, Japan) for controlled positioning of CF tips onto the cells. The hydraulic manipulator was mounted on top of a piezotranslator (P-623.1CL; Precision Instruments GmbH, Karlsruhe, Germany), which was fixed on sleighs of a railing system for coarse positioning (IonOptix, Milton, MA, USA) and controlled by a custom written LabView™ script to allow accurate application of mechanical loads (Iribe et al., 2009).

To track cell movement, CF positions and sarcomere length (SL) were continuously recorded in real-time using the Edge Length and SL detection capabilities of IonWizard (IonOptix).

2.2.1. CF distance and SL detection

CF distance was established by tracking the pronounced contrast between the two individual CF and background (Fig. 2A and B). Noise levels were reduced by using a moderately overexposed camera setting, such that smaller intensity gradients would not be detected by the software.

The two CF do enclose an area which is representative for cell contraction, including periods of altered pre- and afterload.

SL detection is also based on summing up light intensity over Y at every point X within an analysis window overlayed on the cell, making cell alignment an important determinant of signal-to-noise ratio (Fig. 3A). Instead of tracking the derivative of a single contrast, real-time SL measurement uses a fast Fourier transform of the cardiomyocyte striation pattern frequency power spectrum.

To characterise cell contraction and relaxation events (transients), several contractile parameters are used, as shown in Fig. 3B. Time to peak contraction (TTP) corresponds to the duration of the active shortening, measured from the time of field stimulation to maximum shortening, time to relaxation (TTRel) corresponds to the duration from peak shortening to 90% relaxation (near-return to resting sarcomere length; RSL). The negative and positive maxima of the first derivative of length changes during contraction and relaxation give the maximum velocity of contraction (VmaxCon) and the maximum velocity of relaxation (VmaxRel), respectively. Fractional sarcomere shortening (FSS) is the peak amplitude of shortening expressed as a percentage of RSL.

Use of a second camera allows one to optimize the image for SL detection independently of the overexposed CF detection mode.

2.2.2. End-systolic and end-diastolic stress-length relations

After attachment of two CF, the piezo motors will move the two CF to increase preload, usually in 2 μm-steps (within 300 ms per step). By subtracting the observed increase in CF tip distance (Edge Length analysis) from the amount of piezo actuator movement applied, one obtains a measure for CF bending that is caused by passive cell stiffness. Multiplying this with CF stiffness provides the value of passively applied end-diastolic force. This can be plotted as a function of diastolic stretch (to give the end diastolic force-length relation).

Within physiological limits, an increase in preload gives rise to stronger cell contractions, due to the Frank-Starling mechanism. By tracking CF positions, maximum shortening can be quantified, and

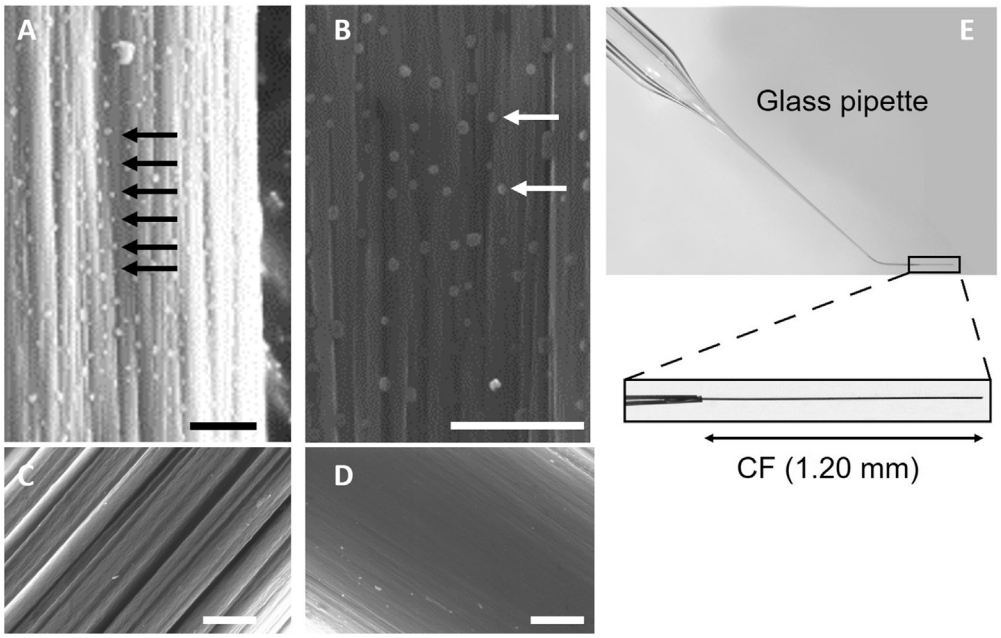

Fig. 1. CF surface and CF holder design. A–D: Scanning electron microscopic images of different CF, scale bars = 1 μm. A: Detail of the surface of a CF from Prof Jean-Yves LeGuennec, B: Same at higher magnification. Arrows show microstructures typical seen on these fibres. C: and D: non-sticky carbon fibres. E: Pulled and bent capillaries used to hold CF.

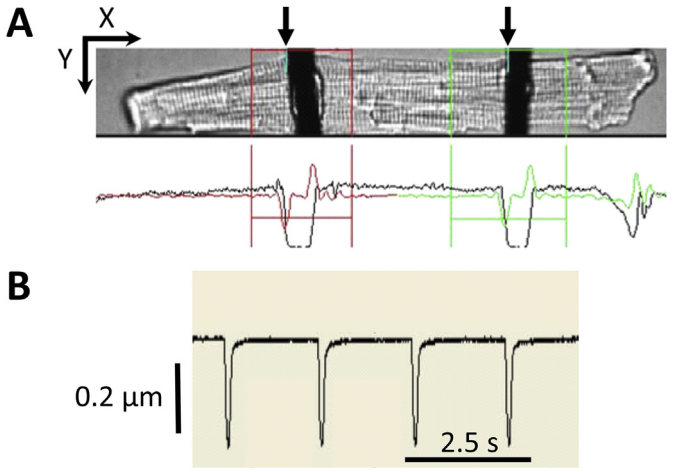

Fig. 2. CF position tracking with the EdgeLength detection system. A: The picture from the camera (top) as displayed by IonWizard software. CF positions are analysed in user-defined windows (red and green boxes) through threshold detection. The black trace underneath the photographic image represents light intensity, summed up over Y for all X positions. The red and green traces show the first derivative, with minima showing bright-to-dark transition (from left) and maxima - dark-to-bright. By defining a threshold (see colour-coded horizontal line cutting across first derivative) one can track the CF edge (here left edge; see arrows. Scale arrows = 25 μm. B) Changes in distance between CF are visualised for further analysis. A mouse cardiomyocyte is shown.

the associated active end-systolic force can be calculated by multiplying CF stiffness with amount of active shortening, i.e. the difference between end-diastolic and end-systolic CF distances. End-systolic force, plotted as a function of end-systolic length, yields the end-systolic force-length relation of auxotonic contractions at different preloads.

Comparisons of contractile activity between cells normally requires normalisation for cell cross sectional area (to normalise absolute force values), and to the length enclosed between the two CF (to normalise absolute length changes). The cross-section area is usually calculated, assuming an elliptical cell cross-section (Anversa and Olivetti, 2011; Wu et al., 2000), where cell thickness is 1/3 of cell width (Nishimura et al., 2004). As force can now be expressed per unit of cell cross-section, force-length relations become end-diastolic and end-systolic stress-length relations: EDSLR and ESSLR, respectively. As, the estimation of cell cross-section is error-prone, we use the dimensionless Frank-Starling Gain (FSG) index, introduced by Bollensdorff et al. (2011), to compare the preload-induced increase in cell contractility between samples. As the FSG divides the slope end-systolic by the slope of end-diastolic behaviour, any errors in assessment of cell cross-section 'are divided out'. For in-depth explanation of EDSLR, ESSLR and FSG index calculations, please see Bollensdorff et al. (2011)

2.3. Perfusion

Unless otherwise stated, cells were superfused (gravity fed) at 2.1 mL/min (chamber volume ~0.7 mL, i.e. equivalent to three solution changes per min), with a physiological, carbogen-bubbled solution containing (in mM): NaCl 137, KCl 5.4, $MgSO_4$ 1.3, Na_2HPO_4 1.2, HEPES 20, $CaCl_2$ 1.8, glucose 15 (pH 7.4). The perfusion chamber (RC27-NE2, Warner Instruments, Hamden, USA) uses a glass coverslip coated with poly-HEMA (2-hydroxyethyl methacrylate; Sigma, Poole, UK) to prevent cell adhesion and minimize friction of mechanically unloaded contractions. Cells were paced at 2 Hz (unless otherwise stated) with 1.5 times the threshold voltage of field stimulation (established separately for each individual cell, usually 10–20 V) using a MyoPacer stimulator (IonOptix). Solution swichting was controlled using a solenoid pinch–valve system (cFlow-V2.x; Cell MicroControls; Norfolk, VA, USA). When working at 37 °C, temperature was controlled *via* a flow-through and a chamber heater, using a two-channel controller (TC-344B; Warner Instruments). After adding cells to the chamber, 10–15 min were allowed for cardiomyocytes to recover and stabilise before recordings were initiated. When perfusing apelin, recordings were taken 5 min after apelin application.

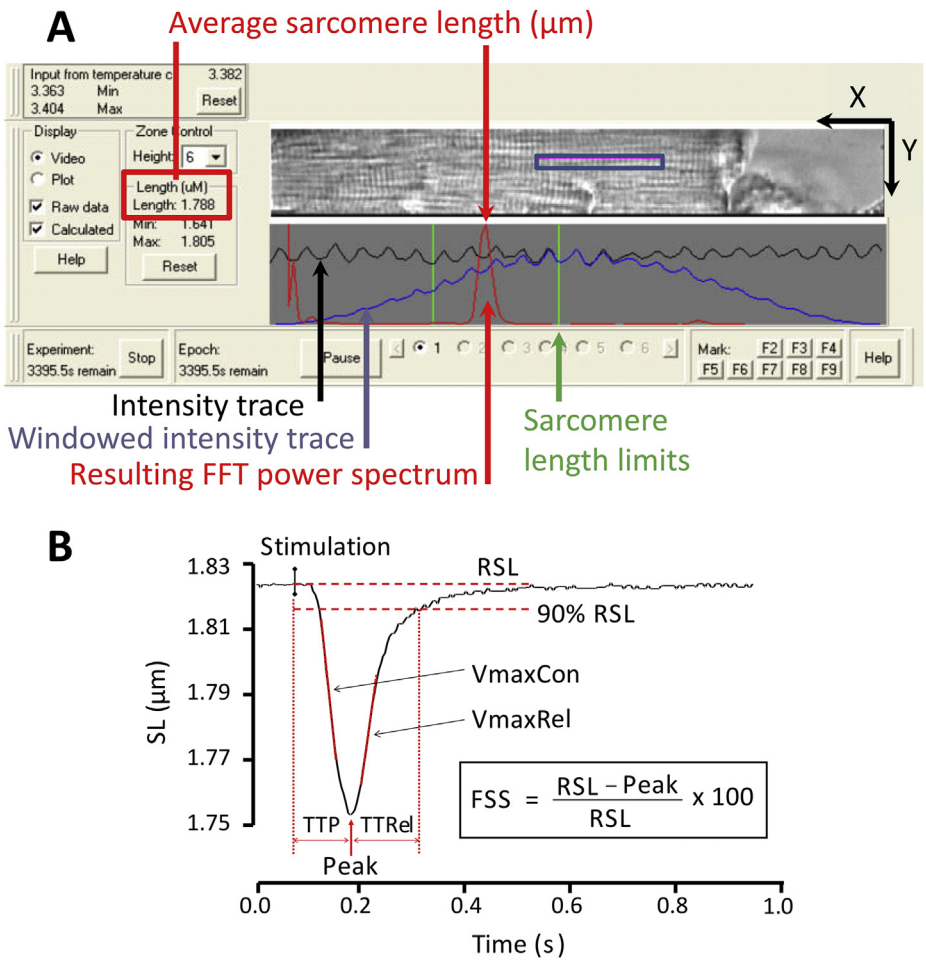

Fig. 3. SL recording interface and contractile parameters analysed. A) IonWizard display used for measuring SL. The detection is based on tracking contrast changes (pixel intensity, summed along Y for each position X in the analysis window) coupled to a fast Fourier transform (FFT). The FFT spectrum (tall and narrow) shown allows one to assess the quality of acquisition. Scale arrows = 25 µm. B) Contractile parameters used to characterise sarcomere contraction transients. These parameters are obtained after analysis with IonWizard. RSL: resting sarcomere length; FSS: fractional sarcomere shortening; TTP: time to peak, TTRel: time to 90% relaxation, VmaxCon: maximum velocity of contraction, VmaxRel: maximum velocity of relaxation. A mouse cardiomyocyte is shown.

2.4. Exclusion criteria for cell selection

Cells exhibiting any of the following criteria were not included in this study: i) lack of clear sarcomeric striations, ii) presence of membrane blebs, iii) spontaneous or local contractions, iv) resting SL < 1.7 µm, v) inability to follow field pacing.

2.5. Statistical analysis

Values are expressed as mean ± standard error of the mean (S.E.M.). Analyses were performed using OriginPro. Differences across groups were evaluated by one way ANOVA with $P < 0.05$ taken to indicate a significant difference between means ($P < 0.05 = *$, $P < 0.01 = **$ and $P < 0.001 = ***$). N-numbers refer to the number of hearts (cell isolations), n-numbers to the number of cells assessed. For conditions with n < 30, significance of the difference between means was tested with a permutation test (R Development Core Team: http://www.r-project.org/).

3. Results

3.1. Apelin effects on freely contracting cells

Apelin, applied at a concentration of 10 nM to the superfusate of isolated, freely-contracting cells in a dish coated to prevent cell adhesion, increases FSS by 8 ± 2% ($p < 0.001$, N = 18, n > 40 for all observations), VmaxCon by 15 ± 2% ($p < 0.001$, N = 18) and VmaxRel by 18 ± 3% ($p < 0.001$, N = 18) without affecting RSL ($p = 0.80$, N = 18) of control wild type (WT) mice (Fig. 4A). In keeping with these changes, TTP and TTRel are significantly reduced (by 10 ± 1% and 11 ± 1%, respectively; both $p < 0.001$, N = 18).

To assess the specificity of the response, apelin was applied to cardiomyocytes isolated from APJ-KO mice (N = 5, n > 40 for all observations). Here, no significant change in any of the recorded parameters was observed (see Fig. 4B for a selection of data).

To assess potential species-dependent effects and to compare with previous reports on rat cells, we carried out a sub-study on rat ventricular myocytes (37 °C, 1 Hz field stimulation: Fig. 5). Apelin increased VmaxCon by 14 ± 5% ($p < 0.05$, N = 6, n > 40 for all observations) and VmaxRel by 24 ± 5% ($p < 0.01$, N = 6, n > 40 for all parameters), but did not induce a significant change in either RSL or FSS ($p > 0.15$, N = 6). TTP and TTRel were significantly decreased (by 11 ± 2% and 21 ± 2%, respectively; both $p < 0.01$, N = 6).

To assess possible effects of temperature or pacing rate, which were major differences between previous single-cell investigations (Farkasfalvi et al., 2007; Wang et al., 2008), we investigated cell responses to apelin at different temperatures (24±2 °C *vs.* 37±2 °C)

and stimulation rates (1 *vs.* 2 Hz) in mouse cells. Neither condition had significant effects on cellular responses of freely-contracting cells to apelin (N = 6, n > 40 for all observations), as shown in Fig. 6.

3.2. Apelin effect on mechanically loaded cells

We explored whether application of a mechanical preload could reveal further effects of apelin on mouse cardiomyocytes. WT cells were stretched, using CF, and ESSLR and EDSLR slopes were calculated (Fig. 7A). The FSG (ESSLR slope divided by EDSLR slope) was used to quantify preload-induced increase in cell contractility (Fig. 7B). Apelin did not change ESSLR slope Fig. 7C, but it decreased EDSLR slope in 12 out of 17 cells tested (70% of tested cells, Fig. 7D).

Because EDSLR slopes and FSG index values obtained were quite scattered, we suspected that endogenous apelin levels or apelin responsiveness may be variable under control conditions. Indeed, endogenous apelin can be increased due to ischemic conditions (Yang et al., 2015), which may occur to a variable extent during cell isolations and/or storage.

To circumvent such variability, similar experiments were repeated on cells isolated from Apelin-KO mice (Fig. 8). In cells isolated from these mice, mean ESSLR slope remained not significantly different, but the mean EDSLR slope was reduced from 242.9 ± 89.8 mN/mm^2 per % cell deformation (N = 6, n = 10) in control conditions to 151.3 ± 28.7 mN/mm^2 per % cell deformation (N = 6, n = 6) in the presence of 10 nM apelin (Fig. 8A). As a result, the FSG index was significantly (p = 0.022) increased in the presence of apelin, from 1.36 ± 0.05 (N = 6, n = 10) to 1.96 ± 0.23 (N = 6, n = 6; Fig. 8C). Also, data obtained in control conditions were much less scattered, with no FSG values exceeding 2. Fig. 8C gives the details of EDSLR slopes for each cells. Without apelin application, the FSG obtained from WT cells was not different from that observed in Apelin-KO cells (Supplementary Fig. 1A).

The enhanced visibility of exogenous apelin effects in apelin-deficient cells is further illustrated by analysis of contractile parameters such as TTP, VmaxCon, VmaxRel in mechanically loaded cells (Fig. 9): Apelin-KO cells show an order of magnitude more pronounced responses to apelin, compared to WT. No difference was observed between the two genotypes without apelin perfusion (Supplementary Fig. 1B) which confirms data in an earlier publication (Charo et al., 2009).

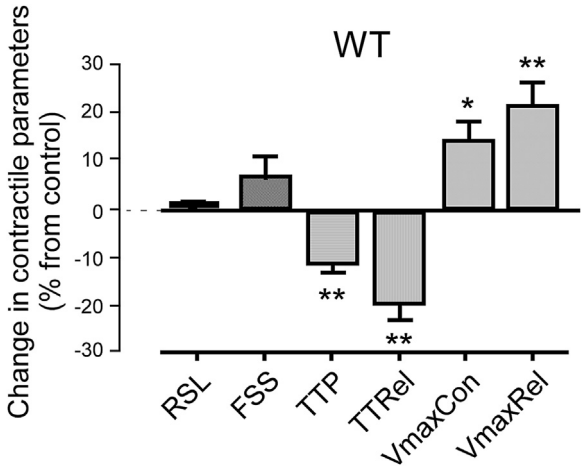

Fig. 5. Apelin (10 nM) effects on contractile parameters in freely contracting rat cardiomyocytes, paced at 1 Hz. N = 6, n > 40 per condition. Unpaired experiments.

4. Discussion

This study shows that apelin speeds up contraction dynamics (TTP, TTRel, VmaxCon and VmaxRel) without affecting RSL of mechanically unloaded WT mouse and rat cardiomyocytes. This response is seen independently of environmental temperature (24 *vs.* 37 °C) and pacing rate (1 Hz *vs.* 2 Hz). Cells from the APJ-KO mice do not respond to apelin application, confirming specificity of the effect which appears to be mediated *via* the apelin receptor. In terms of contractility, apelin application increases FSS in mechanically unloaded WT mouse, but not rat, cells; difference which could be due to species specificities, or possibly effects of differences in enzymes used for cell isolation (collagenase for mice *vs.* liberase for rats). In mechanically preloaded WT mouse cells, apelin does not alter ESSLR, while in 70% of cells, the slope of EDSLR is reduced. Due to high background variability, this does not manifest itself in an increase in group-averaged FSG. We hypothesised that this variability stems, in part at least, from the confounding effects of differences in endogenous apelin levels. To address this issue, we used cardiomyocytes isolated from Apelin-KO mice. Here, apelin application gave rise to a significant increase in FSG, driven by a

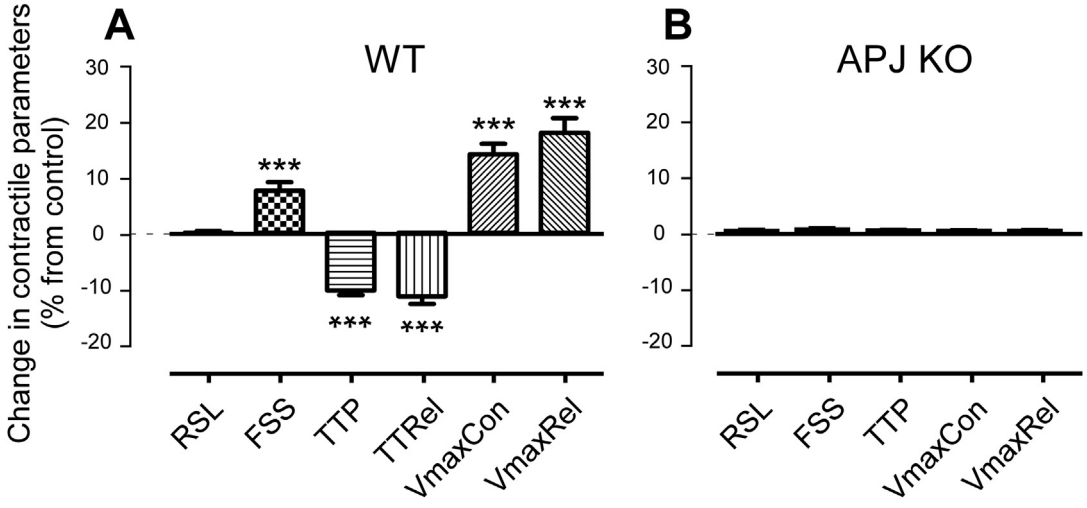

Fig. 4. Apelin (10 nM) effects on contractile parameters of freely contracting cardiomyocytes, isolated from control, N = 18, n > 40 for each condition and for each N (A) and APJ-KO (B) mice (N = 5 each for control and APJ-KO; n = 69 for apelin-free and n = 53 for apelin-exposed condition). Unpaired experiments.

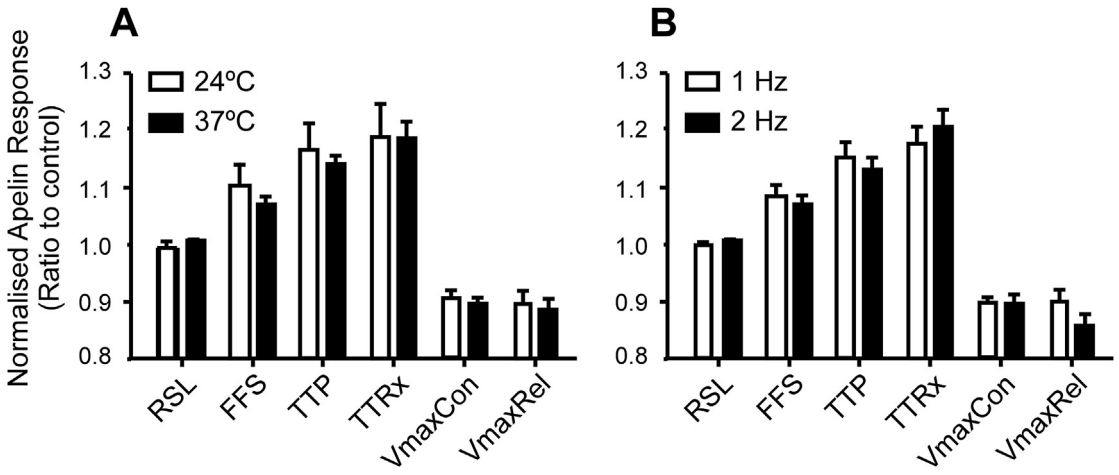

Fig. 6. Changes in temperature and pacing rate do not alter apelin (10 nM) effects on contractile parameters in freely contracting cells, seeded on a non-stick surface. A) Contractile response to apelin in isolated, field stimulated wild-type murine ventricular myocytes at different temperatures (N = 12 at 37 ± 2 °C and 6 at 24 ± 2 °C, n > 40 per condition). B) Contractile response to apelin at different pacing rates (N = 12 at 1 Hz and 6 at 2 Hz, n > 40 per condition). Unpaired experiments.

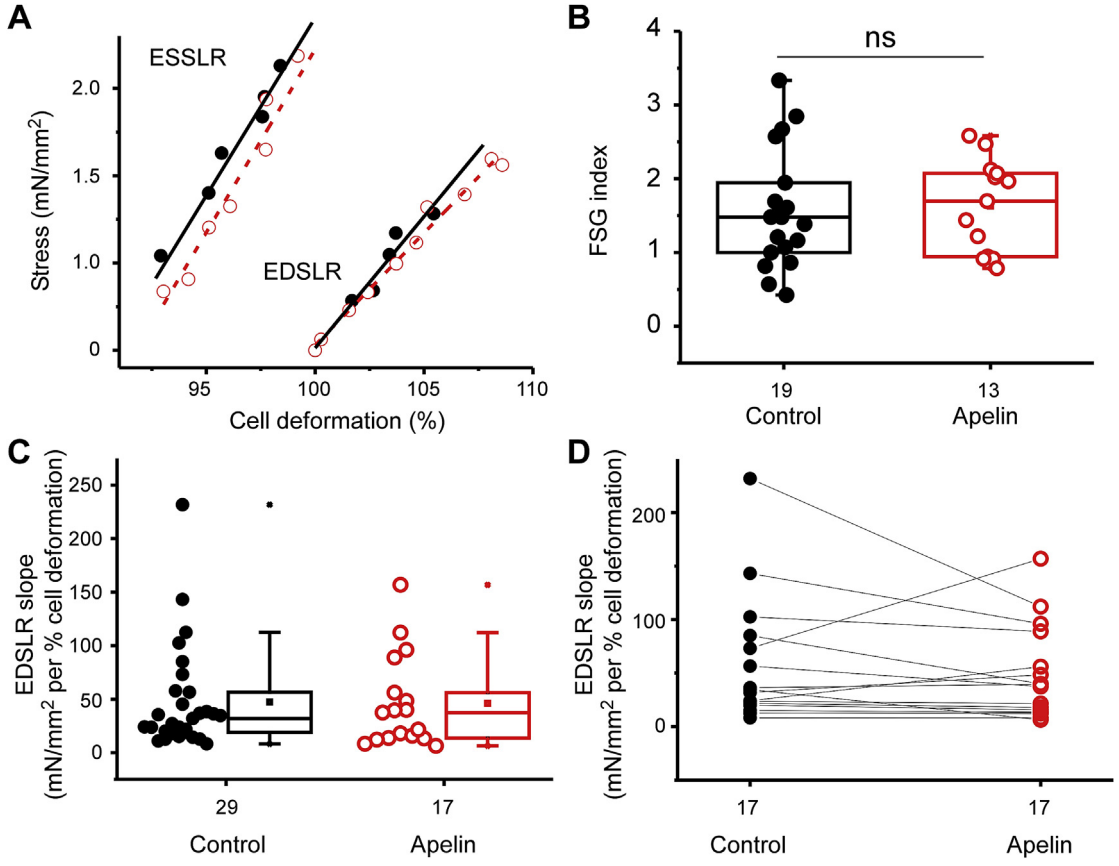

Fig. 7. Apelin (10 nM) effect on Frank-Starling-Gain (FSG) in WT cells. A) ESSLR and EDSLR slopes from a representative cell in control conditions (black solid line) and in the presence of apelin (red dashed line). B) Effect of apelin perfusion on FSG (N = 8; n-numbers shown in figure, unpaired data). C) Effect of apelin perfusion on EDSLR slope values (N = 14; n-numbers shown in figure, unpaired data). D) EDSLR slopes values before and after apelin perfusion, paired experiments (N = 8; n = 17).

reduction in EDSLR – i.e. by a positive lusitropic effect. This pre-load induced lusitropy-driven increase in contractility was confirmed in mechanically afterloaded Apelin-KO cell contraction dynamics, where apelin-induced changes in TTP, TTRel, VmaxCon and VmaxRel were an order of magnitude larger than in WT cardiomyocytes.

The results of our study show that controlling the mechanical environment of isolated cells may help unravel drug effects which would be hidden in freely contracting cells. When freely contracting, cells in presence of apelin show a shorter end-systolic sarcomere length while RSL is unchanged. The reason for this is that mechanically unloaded cells experience no force that would reveal an increased diastolic compliance, hence no change in RSL. In auxotonic conditions (here using the CF technique), cells

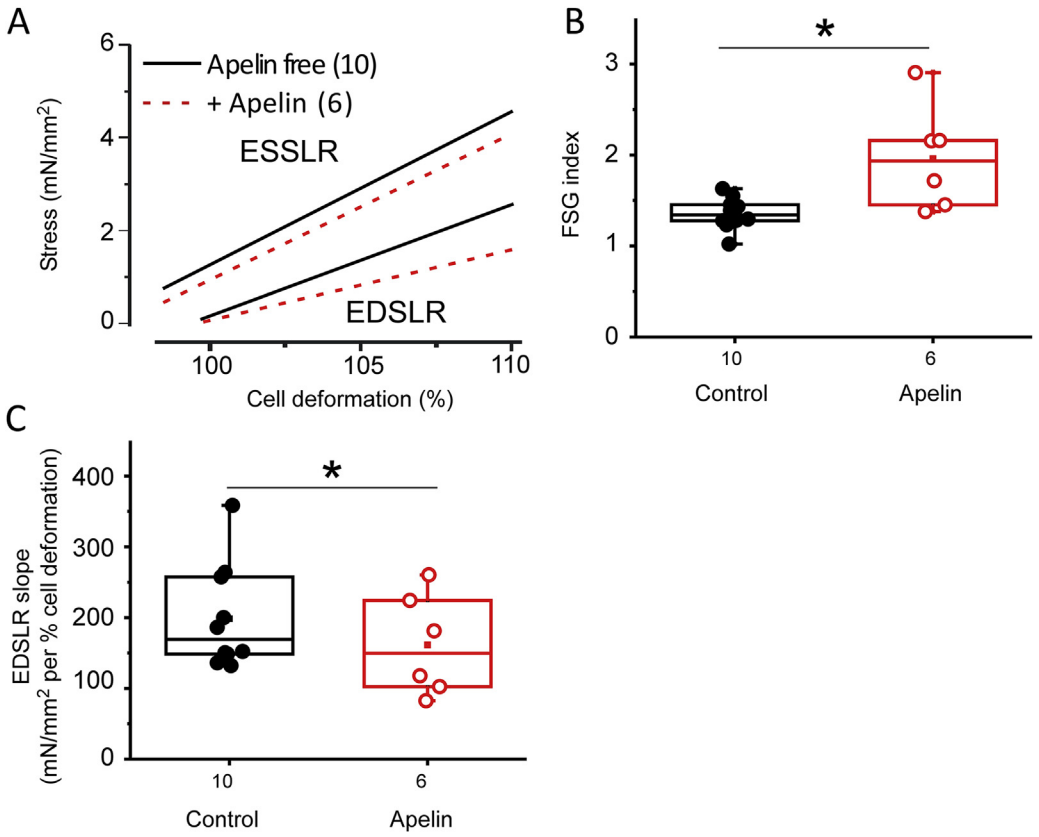

Fig. 8. Apelin (10 nM) effect on preload dependent contractile behaviour of apelin-deficient cells. A) Mean ESSLR and EDSLR in the absence (black) or presence (red) of apelin in Apelin-KO cells. B) Apelin effect on FSG in cells from Apelin-KO mice. C) Apelin causes a significant reduction in EDSLR slopes (i.e. a positive lusitropic effect). N = 6; for n-numbers – see figure.

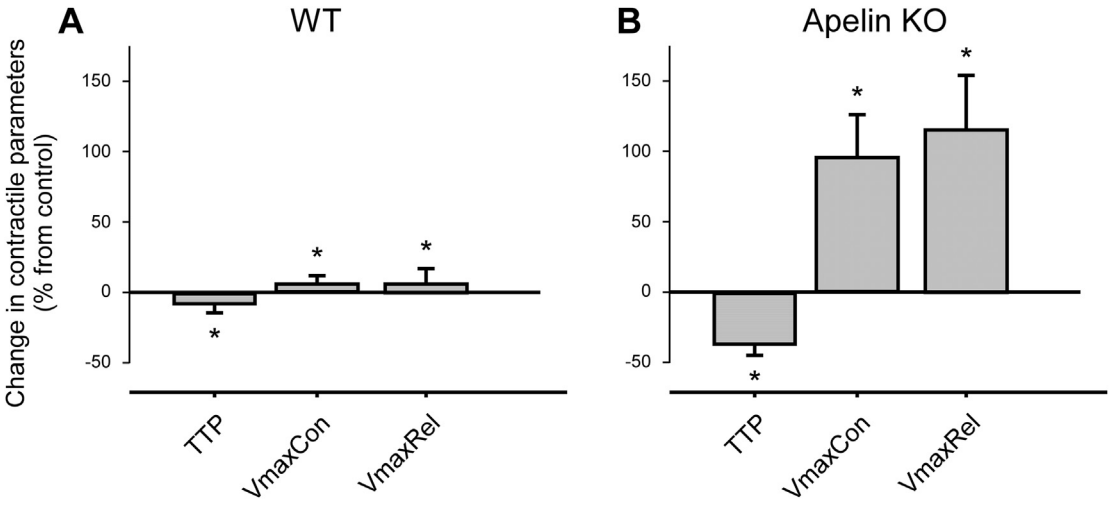

Fig. 9. Apelin (10 nM) effects on key mechanical parameters in afterloaded cardiomyocytes, isolated from A) WT and B) Apelin-KO mice. WT: N = 9, n = 17 for control and for apelin application. Apelin-KO: N = 4, n = 11 for control and n = 7 for apelin application.

experience such a diastolic preload. This reveals the key apelin effect: while end-systolic sarcomere length is not significantly changed anymore (compared to control conditions), end-diastolic RSL is (Fig. 8A).

End diastolic length-stress is a measure of cardiac compliance, or rather of passive force, whilst the end-systolic length-stress is a measure of total force (Bollensdorff et al., 2011). In our study, there is a reduction in EDSLR, indicating an increased compliance of the cardiomyocyte. This is not accompanied by a change in ESSLR. Therefore, while there is no change in total force, active force of contraction is increased on the background of a reduction in passive force This effect increases with stretch/preload. The mechanisms governing these responses need not be the same and, in fact, the range of proteins now implicated as effectors of apelin signalling, as

well as G-protein mediated cascades, suggest that multiple pathways may contribute to the physiological response.

Determinants of compliance in the heart are not fully understood. In isolated myocytes changes in extracellular matrix properties can not be considered. Different titin isoforms (Methawasin et al., 2014), as well as titin phosphorylation by protein kinase (PK) A, PKG and PKC (Fukuda et al., 2010), alter cardiac compliance. Previous work has suggested that apelin induces changes in inotropy partially *via* a PKC-dependent mechanism (Szokodi et al., 2002b; Chamberland et al., 2010) and partially *via* the G protein G_i (Szokodi et al., 2002b). These two pathways, however, have not accounted for the complete response and further mechanistic studies are needed. Two papers have highlighted a role for sodium-hydrogen exchange in apelin-mediated increases in contractility (Farkasfalvi et al., 2007; Szokodi et al., 2002b). Rapid effects of apelin have been observed without concurrent changes in the calcium transient. It has also been reported that around 50% of the response to apelin is abolished after inhibition of myosin light chain kinase (MLCK) (Perjés et al., 2014). MLCK phosphorylation is associated with an increase calcium sensitivity of the myofibrils and accelerated kinetics of crossbridge formation through phosphorylation of the regulatory light chain (Colson et al., 2010); it is possible that this mechanism underlies the responses seen in our study.

The apelin gene is located on the X-chromosome, and one could wonder whether the differential representation of sex chromosome genes within male *vs*. female cells could affect the phenotype. Traditionally, the answer to the question is no, as most X genes are expressed at a similar level in males and females. This is because one X chromosome is inactivated in each XX female cell, so that only one X chromosome is active in cells of both sexes. However, some X genes escape this X-inactivation, and are expressed higher in XX than XY cells (Brown and Greally, 2003). Such genes can then cause sex differences due to their double representation in the genome of XX cells. In our study we used males exclusively to ascertain reliably comparable apelin expression in cells from different animals and to avoid hormonal effects. However, the question of potential sex differences in apelin signalling is an interesting and important one, albeit beyond the scope of this manuscript.

Mechano-sensitivity of drug actions is an important and under-investigated facet of pharmacology. This may give rise both to false-positive and false-negative observations *in vitro*, where either cardiac side-effects or beneficial actions may be missed.

In the given case, a false-negative interpretation of apelin effects could have occurred, if contractions had been studied in standard cardiac perfusion chambers (which tend to be furnished with a 'sticky' coating to keep cells in position – an approach that alters the mechanical environment and would be expected to reduce apelin effects on cell contraction parameters such as FSS). This is of particular importance when considering end-diastolic and end-systolic sarcomere lengths. Use of a non-stick perfusion dish, and analysis of dynamic contraction parameters (such as TTP, TTRel, VmaxCon and VmaxRel) is needed to get meaningful data in spite of high variability seen in WT cells.

Apelin provides an exciting motif for mechano-sensitive pharmacological interventions that target stretched myocardium, *i.e.* tissue which is not able to contract as strongly as neighbouring myocardium. The fact that it is not the systolic, but rather the diastolic behaviour that appears to be modified by apelin may explain some of the previously reported discrepancies in effects seen at organ and single cell levels. It also underlies the ability of apelin to increase contractility more than the associated energy demand (Charo et al., 2009), making this peptide interesting for therapeutic targeting of cardiac tissue with reduced oxygen and/or energy supply – which, as a rule, will also be stretched, i.e. more sensitive to apelin effects.

Given our assertion regarding apelin effects in stretched myocardium it is interesting to note that several studies have investigated pressure-induced changes and signalling with relation to apelin and APJ. Pressure overload induces a significant upregulation of apelin, whilst apelin KO mice are more susceptible to heart failure after pressure overload (Kuba et al., 2007). Stretch of cultured neonatal rat ventricular myocytes has been reported both to upregulate (Xie et al., 2014) or downregulate (Szokodi et al., 2002b) APJ expression. APJ shares ~50% sequence homology with the angiotensin type II receptor AT1 (O'Dowd et al., 1993) and, similarly, APJ appears to be mechanosensitive in its own right. A study using freshly isolated and neonatal cultured rat ventricular cardiomyocytes indicate that stretch could directly stimulate APJ (Scimia et al., 2012), and that APJ KO mice appear to be protected from hypertrophy, heart failure and reduced fractional shortening associated with trans-aortic constriction (TAC; a pressure overload model to induce heart failure), whilst apelin KO mice exhibited greater hypertrophy after TAC (Scimia et al., 2012). It has also been suggested using a culture model that pressure-induced myocyte hypertrophy requires APJ expression and occurs *via* activation of PI3K-autophagy pathway (Xie et al., 2014). It should be noted, however, that the mechanosensitive effects discussed refer to stretch for a period of several hours, or even weeks-to-months (in TAC). The effects of acute stretch seen in our experiments (minutes) are unlikely to be confounded by APJ expression changes or activation of autophagic or hypertrophic pathways.

Positive lusitropy is a promising avenue for increasing active cardiac force production without running the risks of established pharmacological interventions that raise intracellular calcium levels, which may lead to calcium overload-induced arrhythmogenesis and which are associated with high energy cost for the cell (Vassalle and Lin, 2004). Positive lusitropy, observed in single cells, might explain earlier counter-intuitive findings of apelin-induced increase in contractility occurring without matching rise in oxygen consumption (Charo et al., 2009). In addition, a therapeutic strategy based on improving relaxation may also prevent or reduce cardiac hypertrophy which is a common side effect of inotropes.

That said, a limitation needs to be considered. As apelin is endogenously expressed, it may be present already in the cells of interest, perhaps even as an emergency response mechanism of the heart to myocardial stress, making endogenous apelin levels difficult to control and exogenously applied apelin potentially less efficient. While apelin itself may not be as effective an interventional tool as one might wish, it still highlights a promising direction of research and development, targeting the diastolic state to improve cardiac contractile function.

5. Conclusion

Apelin-treated myocytes exhibit a preload-dependent increase in contractility, predominantly *via* a positive lusitropic effect enhancing cell relaxation. This is a novel and compelling theme for the development of drug interventions to increase active contraction in weakened myocardium without a matching need to increase energy demand.

Acknowledgements

This research was supported by an Imperial College Junior Research Fellowship to RP and a British Heart Foundation award to CB and PK. EAR-Z was an Immediate Post-Doctoral Fellow of the British Heart Foundation (BHF); PK a Senior Fellow of the BHF. PK acknowledges support by the ERC Advanced Grant CardioNECT (323009). RAC was supported by a BHF graduate studentship.

Appendix A. Supplementary data

Supplementary data related to this article can be found at https://doi.org/10.1016/j.pbiomolbio.2017.09.013.

References

Anversa, P., Olivetti, G., 2011. Cellular basis of physiological and pathological myocardial growth. Compr. Physiol.

Ashley, E.A., Powers, J., Chen, M., Kundu, R., Finsterbach, T., Caffarelli, A., Deng, A., Eichhorn, J., Mahajan, R., Agrawal, R., Greve, J., Robbins, R., Patterson, A.J., Bernstein, D., Quertermous, T., 2005. The endogenous peptide apelin potently improves cardiac contractility and reduces cardiac loading in vivo. Cardiovasc. Res. 65, 73–82.

Beltowski, J., 2006. Apelin and visfatin: unique "beneficial" adipokines upregulated in obesity? Med. Sci. Monit. 12, RA112–R119.

Berry, M.F., Pirolli, T.J., Jayasankar, V., Burdick, J., Morine, K.J., Gardner, T.J., Woo, Y.J., 2004. Apelin has in vivo inotropic effects on normal and failing hearts. Circulation 110, II187–I193.

Bollensdorff, C., Lookin, O., Kohl, P., 2011. Assessment of contractility in intact ventricular cardiomyocytes using the dimensionless 'Frank–Starling Gain'-index. Pflügers Archiv-European J. Physiol. 462, 39–48.

Brown, C.J., Greally, J.M., 2003. A stain upon the silence: genes escaping X inactivation. TRENDS Genet. 19, 432–438.

Bub, G., Camelliti, P., Bollensdorff, C., Stuckey, D.J., Picton, G., Burton, R., Clarke, K., Kohl, P., 2010. Measurement and analysis of sarcomere length in rat cardiomyocytes in situ and in vitro. Am. J. Physiol-Heart Circ. Physiol. 298, H1616–H1625.

Buettner, H.J., Mueller, C., Gick, M., Ferenc, M., Allgeier, J., Comberg, T., Werner, K.D., Schindler, C., Neumann, F.J., 2007. The impact of obesity on mortality in UA/non-ST-segment elevation myocardial infarction. Eur. Heart J. 28, 1694–1701.

Chamberland, C., Barajas-Martinez, H., Haufe, V., Fecteau, M.-H., Delabre, J.-F., Burashnikov, A., Antzelevitch, C., Lesur, O., Chraibi, A., Sarret, P., 2010. Modulation of canine cardiac sodium current by Apelin. J. Mol. Cell. Cardiol. 48, 694–701.

Charles, C.J., Rademaker, M.T., Richards, A.M., 2006. Apelin-13 induces a biphasic haemodynamic response and hormonal activation in normal conscious sheep. J. Endocrinol. 189, 701–710.

Charo, D.N., Ho, M., Fajardo, G., Kawana, M., Kundu, R.K., Sheikh, A.Y., Finsterbach, T.P., Leeper, N.J., Ernst, K.V., Chen, M.M., 2009. Endogenous regulation of cardiovascular function by apelin-APJ. Am. J. Physiol. Heart Circ. Physiol. 297, H1904–H1913.

Chen, M.M., Ashley, E.A., Deng, D.X., Tsalenko, A., Deng, A., Tabibiazar, R., Ben-Dor, A., Fenster, B., Yang, E., King, J.Y., 2003. Novel role for the potent endogenous inotrope apelin in human cardiac dysfunction. Circulation 108, 1432–1439.

Chen, Z., Wu, D., Li, L., Chen, L., 2016. Apelin/APJ system: a novel therapeutic target for myocardial ischemia/reperfusion injury. DNA Cell Biol. 35, 766–775.

Cheng, X., Cheng, X.S., Pang, C.C., 2003. Venous dilator effect of apelin, an endogenous peptide ligand for the orphan APJ receptor, in conscious rats. Eur. J. Pharmacol. 470, 171–175.

Cheng, C.C., Weerateerangkul, P., Lu, Y.Y., Chen, Y.C., Lin, Y.K., Chen, S.A., Chen, Y.J., 2013. Apelin regulates the electrophysiological characteristics of atrial myocytes. Eur. J. Clin. Investig. 43, 34–40.

Colson, B.A., Locher, M.R., Bekyarova, T., Patel, J.R., Fitzsimons, D.P., Irving, T.C., Moss, R.L., 2010. Differential roles of regulatory light chain and myosin binding protein-C phosphorylations in the modulation of cardiac force development. J. Physiol. 588, 981–993.

Farkasfalvi, K., Stagg, M.A., Coppen, S.R., Siedlecka, U., Lee, J., Soppa, G.K., Marczin, N., Szokodi, I., Yacoub, M.H., Terracciano, C.M., 2007. Direct effects of apelin on cardiomyocyte contractility and electrophysiology. Biochem. Biophys. Res. Commun. 357, 889–895.

Folino, A., Montarolo, P.G., Samaja, M., Rastaldo, R., 2015. Effects of apelin on the cardiovascular system. Heart Fail. Rev. 20, 505–518.

Fukuda, N., Terui, T., Ishiwata, Si, Kurihara, S., 2010. Titin-based regulations of diastolic and systolic functions of mammalian cardiac muscle. J. Mol. Cell. Cardiol. 48, 876–881.

Higuchi, K., Masaki, T., Gotoh, K., Chiba, S., Katsuragi, I., Tanaka, K., Kakuma, T., Yoshimatsu, H., 2007. Apelin, an APJ receptor ligand, regulates body adiposity and favors the messenger ribonucleic acid expression of uncoupling proteins in mice. Endocrinology 148, 2690–2697.

Hosoya, M., Kawamata, Y., Fukusumi, S., Fujii, R., Habata, Y., Hinuma, S., Kitada, C., Honda, S., Kurokawa, T., Onda, H., 2000. Molecular and functional characteristics of APJ tissue distribution of mRNA and interaction with the endogenous ligand apelin. J. Biol. Chem. 275, 21061–21067.

Iribe, G., Helmes, M., Kohl, P., 2007. Force-length relations in isolated intact cardiomyocytes subjected to dynamic changes in mechanical load. Am. J. Physiol. Heart Circ. Physiol. 292, H1487–H1497.

Iribe, G., Ward, C.W., Camelliti, P., Bollensdorff, C., Mason, F., Burton, R.A., Garny, A., Morphew, M.K., Hoenger, A., Lederer, W.J., Kohl, P., 2009. Axial stretch of rat single ventricular cardiomyocytes causes an acute and transient increase in Ca^{2+} spark rate. Circ. Res. 104, 787–795.

Ishida, J., Hashimoto, T., Hashimoto, Y., Nishiwaki, S., Iguchi, T., Harada, S., Sugaya, T., Matsuzaki, H., Yamamoto, R., Shiota, N., Okunishi, H., Kihara, M., Umemura, S., Sugiyama, F., Yagami, K., Kasuya, Y., Mochizuki, N., Fukamizu, A., 2004. Regulatory roles for APJ, a seven-transmembrane receptor related to angiotensin-type 1 receptor in blood pressure in vivo. J. Biol. Chem. 279, 26274–26279.

Kagiyama, S., Fukuhara, M., Matsumura, K., Lin, Y., Fujii, K., Iida, M., 2005. Central and peripheral cardiovascular actions of apelin in conscious rats. Regul. Pept. 125, 55–59.

Kawamata, Y., Habata, Y., Fukusumi, S., Hosoya, M., Fujii, R., Hinuma, S., Nishizawa, N., Kitada, C., Onda, H., Nishimura, O., 2001. Molecular properties of apelin: tissue distribution and receptor binding. Biochim. Biophys. Acta (BBA)-Cell Res. 1538, 162–171.

Kleinz, M.J., Skepper, J.N., Davenport, A.P., 2005. Immunocytochemical localisation of the apelin receptor, APJ, to human cardiomyocytes, vascular smooth muscle and endothelial cells. Regul. Pept. 126, 233–240.

Kuba, K., Zhang, L., Imai, Y., Arab, S., Chen, M., Maekawa, Y., Leschnik, M., Leibbrandt, A., Markovic, M., Schwaighofer, J., 2007. Impaired heart contractility in Apelin gene–deficient mice associated with aging and pressure overload. Circ. Res. 101, e32–e42.

Le Guennec, J.Y., Peineau, N., Argibay, J.A., Mongo, K.G., Garnier, D., 1990. A new method of attachment of isolated mammalian ventricular myocytes for tension recording: length dependence of passive and active tension. J. Mol. Cell. Cardiol. 22, 1083–1093.

Lee, D.K., Cheng, R., Nguyen, T., Fan, T., Kariyawasam, A.P., Liu, Y., Osmond, D.H., George, S.R., O'Dowd, B.F., 2000. Characterization of apelin, the ligand for the APJ receptor. J. Neurochem. 74, 34–41.

Lee, D.K., Saldivia, V.R., Nguyen, T., Cheng, R., George, S.R., O'Dowd, B.F., 2005. Modification of the terminal residue of apelin-13 antagonizes its hypotensive action. Endocrinology 146, 231–236.

Lee, D.K., George, S.R., O'Dowd, B.F., 2006. Unravelling the roles of the apelin system: prospective therapeutic applications in heart failure and obesity. Trends Pharmacol. Sci. 27, 190–194.

Louch, W.E., Sheehan, K.A., Wolska, B.M., 2011. Methods in cardiomyocyte isolation, culture, and gene transfer. J. Mol. Cell. Cardiol. 51, 288–298.

Maguire, J.J., Kleinz, M.J., Pitkin, S.L., Davenport, A.P., 2009. [Pyr1] Apelin-13 identified as the predominant apelin isoform in the human heart. Hypertension 54, 598–604.

Medhurst, A.D., Jennings, C.A., Robbins, M.J., Davis, R.P., Ellis, C., Winborn, K.Y., Lawrie, K.W., Hervieu, G., Riley, G., Bolaky, J.E., 2003. Pharmacological and immunohistochemical characterization of the APJ receptor and its endogenous ligand apelin. J. Neurochem. 84, 1162–1172.

Mesmin, C., Fenaille, Fo, Becher, Fo, Tabet, J.-C., Ezan, E., 2011. Identification and characterization of apelin peptides in bovine colostrum and milk by liquid chromatography–mass spectrometry. J. proteome Res. 10, 5222–5231.

Methawasin, M., Hutchinson, K.R., Lee, E.-J., Smith, J.E., Saripalli, C., Hidalgo, C.G., Ottenheijm, C.A., Granzier, H., 2014. Experimentally increasing titin compliance in a novel mouse model attenuates the Frank-Starling mechanism but has a beneficial effect on diastole. Circulation 113.

Nishimura, S., Yasuda, S-i, Katoh, M., Yamada, K.P., Yamashita, H., Saeki, Y., Sunagawa, K., Nagai, R., Hisada, T., Sugiura, S., 2004. Single cell mechanics of rat cardiomyocytes under isometric, unloaded, and physiologically loaded conditions. Am. J. Physiol-Heart C 287, H196–H202.

O'Carroll, A.-M., Lolait, S.J., Harris, L.E., Pope, G.R., 2013. The apelin receptor APJ: journey from an orphan to a multifaceted regulator of homeostasis. J. Endocrinol. 219, R13–R35.

O'Dowd, B.F., Heiber, M., Chan, A., Heng, H.H., Tsui, L.-C., Kennedy, J.L., Shi, X., Petronis, A., George, S.R., Nguyen, T., 1993. A human gene that shows identity with the gene encoding the angiotensin receptor is located on chromosome 11. Gene 136, 355–360.

O'Shea, M., Hansen, M.J., Tatemoto, K., Morris, M.J., 2003. Inhibitory effect of apelin-12 on nocturnal food intake in the rat. Nutr. Neurosci. 6, 163–1667.

Perjés, Á., Skoumal, R., Tenhunen, O., Kónyi, A., Simon, M., Horváth, I.G., Kerkelä, R., Ruskoaho, H., Szokodi, I., 2014. Apelin increases cardiac contractility via protein kinase Cε-and extracellular signal-regulated kinase-dependent mechanisms. PLoS One 9, e93473.

Ronkainen, V.P., Ronkainen, J.J., Hänninen, S.L., Leskinen, H., Ruas, J.L., Pereira, T., Poellinger, L., Vuolteenaho, O., Tavi, P., 2007. Hypoxia inducible factor regulates the cardiac expression and secretion of apelin. FASEB J. 21, 1821–1830.

Scimia, M.C., Hurtado, C., Ray, S., Metzler, S., Wei, K., Wang, J., Woods, C.E., Purcell, N.H., Catalucci, D., Akasaka, T., 2012. APJ acts as a dual receptor in cardiac hypertrophy. Nature 488, 394.

Seyedabadi, M., Goodchild, A.K., Pilowsky, P.M., 2002. Site-specific effects of apelin-13 in the rat medulla oblongata on arterial pressure and respiration. Auton. Neurosci. 101, 32–38.

Simpkin, J.C., Yellon, D.M., Davidson, S.M., Lim, S.Y., Wynne, A.M., Smith, C.C., 2007. Apelin-13 and apelin-36 exhibit direct cardioprotective activity against ischemiareperfusion injury. Basic Res. Cardiol. 102, 518–528.

Szokodi, I., Tavi, P., Földes, G., Voutilainen-Myllyla, S., Ilves, M., Tokola, H., Pikkarainen, S., Piuhola, J., Rysa, J., Toth, M., Ruskoaho, H., 2002. Apelin, the novel endogenous ligand of the orphan receptor APJ, regulates cardiac contractility. Circ. Res. 91, 434–440.

Szokodi, I., Tavi, P., Földes, G., Voutilainen-Myllylä, S., Ilves, M., Tokola, H., Pikkarainen, S., Piuhola, J., Rysä, J., Tóth, M., 2002. Apelin, the novel endogenous ligand of the orphan receptor APJ, regulates cardiac contractility. Circ. Res. 91, 434–440.

Tatemoto, K., Hosoya, M., Habata, Y., Fujii, R., Kakegawa, T., Zou, M.X., Kawamata, Y.,

Fukusumi, S., Hinuma, S., Kitada, C., Kurokawa, T., Onda, H., Fujino, M., 1998. Isolation and characterization of a novel endogenous peptide ligand for the human APJ receptor. Biochem. Biophys. Res. Commun. 251, 471–476.
Tatemoto, K., Hosoya, M., Habata, Y., Fujii, R., Kakegawa, T., Zou, M.-X., Kawamata, Y., Fukusumi, S., Hinuma, S., Kitada, C., 1998. Isolation and characterization of a novel endogenous peptide ligand for the human APJ receptor. Biochem. Biophys. Res. Commun. 251, 471–476.
Tatemoto, K., Takayama, K., Zou, M.X., Kumaki, I., Zhang, W., Kumano, K., Fujimiya, M., 2001. The novel peptide apelin lowers blood pressure via a nitric oxide-dependent mechanism. Regul. Pept. 99, 87–92.
Vassalle, M., Lin, C.-I., 2004. Calcium overload and cardiac function. J. Biomed. Sci. 11, 542–565.
Walker, S., Danton, M.H., Lang, A.D., Lyall, F., 2014. Apelin receptor (APJ) expression during cardiopulmonary bypass in children undergoing surgical repair. PLoS One 9, e106262.
Wang, C., Du, J.-F., Wu, F., Wang, H.-C., 2008. Apelin decreases the SR Ca 2+ content but enhances the amplitude of [Ca 2+] i transient and contractions during twitches in isolated rat cardiac myocytes. Am. J. Physiol-Heart C 294, H2540–H2546.
Wu, Y., Cazorla, O., Labeit, D., Labeit, S., Granzier, H., 2000. Changes in titin and collagen underlie diastolic stiffness diversity of cardiac muscle. J. Mol. Cell. Cardiol. 32, 2151–2161.
Xie, F., Liu, W., Feng, F., Li, X., Yang, L., Lv, D., Qin, X., Li, L., Chen, L., 2014. A static pressure sensitive receptor APJ promote H9c2 cardiomyocyte hypertrophy via PI3K-autophagy pathway. Acta Biochim. Biophys. Sin. 46, 699–708.
Yang, Y., Lv, S.-Y., Lyu, S.-K., Wu, D., Chen, Q., 2015. The protective effect of apelin on ischemia/reperfusion injury. Peptides 63, 43–46.